THE JOURNAL OF BIOLOGICAL CHEMISTRY Vol. 274, No. 5, Issue of January 29, pp. 3055–3066, 1999
Printed in U.S.A.

AKAP350, a Multiply Spliced Protein Kinase A-anchoring Protein Associated with Centrosomes*

(Received for publication, September 24, 1998)

P. Henry Schmidt‡, Daniel T. Dransfield§, Jaime O. Claudio¶, Robert G. Hawley¶, Kevin W. Trotter‖, Sharon L. Milgram‖, and James R. Goldenring‡§‡‡**

*From the Institute of Molecular Medicine and Genetics, Departments of §Medicine, ‡Surgery, and **Cellular Biology and Anatomy, Medical College of Georgia and the Augusta Veterans Affairs Medical Center, Augusta, Georgia 30912, the ‖Department of Cell and Molecular Physiology, University of North Carolina, Chapel Hill, North Carolina 27599, and the ¶Oncology Gene Therapy Program, The Toronto Hospital and Department of Medical Biophysics, University of Toronto, Toronto, Ontario M5G 2M1, Canada*

Protein kinase A-anchoring proteins (AKAPs) localize the second messenger response to particular subcellular domains by sequestration of the type II protein kinase A. Previously, AKAP120 was identified from a rabbit gastric parietal cell cDNA library; however, a monoclonal antibody raised against AKAP120 labeled a 350-kDa band in Western blots of parietal cell cytosol. Recloning has now revealed that AKAP120 is a segment of a larger protein, AKAP350. We have now obtained a complete sequence of human gastric AKAP350 as well as partial cDNA sequences from human lung and rabbit parietal cells. The genomic region containing AKAP350 is found on chromosome 7q21 and is multiply spliced, producing at least three distinct AKAP350 isoforms as well as yotiao, a protein associated with the *N*-methyl-D-aspartate receptor. Rabbit parietal cell AKAP350 is missing a sequence corresponding to a single exon in the middle of the molecule located just after the yotiao homology region. Two carboxyl-terminal splice variants were also identified. Both of the major splice variants showed tissue- and cell-specific expression patterns. Immunofluorescence microscopy demonstrated that AKAP350 was associated with centrosomes in many cell types. In polarized Madin-Darby canine kidney cells, AKAP350 localized asymmetrically to one pole of the centrosome, and nocodazole did not alter its localization. During the cell cycle, AKAP350 was associated with the centrosomes as well as with the cleavage furrow during anaphase and telophase. Several epithelial cell types also demonstrated noncentrosomal pools of AKAP350, especially parietal cells, which contained multiple cytosolic immunoreactive foci throughout the cells. The localization of AKAP350 suggests that it may regulate centrosomal and noncentrosomal cytoskeletal systems in many different cell types.

Transduction of signals from extracellular stimuli is most commonly accomplished via ligand-receptor binding and generation of a second messenger response. While increases in intracellular second messengers have traditionally been viewed as global cellular events, second messenger effects are often limited to particular regions or organelles within cells. Investigations over the past decade have led to a greater understanding of the mechanisms responsible for the compartmentalization of second messenger effects. These studies have identified a diverse group of scaffolding proteins that sequester both protein kinases and protein phosphatases within specific cellular domains (1, 2). In the case of cAMP-dependent protein kinases, protein kinase A-anchoring proteins (AKAPs)[1] tether the protein kinase A holoenzyme through binding to the regulatory subunit dimer. A growing group of AKAPs that bind the regulatory subunit of type II protein kinase A (R_{II}) have been reported over the past several years. The first R_{II}-binding protein was identified over 15 years ago when microtubule-associated protein 2 (MAP-2) was described (3, 4). Since that time, several AKAPs have been identified, localizing the type II protein kinase A to thyroid cytoskeleton (5), mitochondria (6), the Golgi apparatus (7, 8), centrosomes (8, 9), and microtubules (7, 10), among other places. More recently, an AKAP with binding capacity for the regulatory subunits of type I protein kinase A has also been reported (11).

A number of AKAPs are associated with the cell cytoskeleton and appear to regulate plasma membrane events possibly through anchoring at the sites of interaction between cytoskeletal elements and membrane receptors and channels. Ezrin, a member of the ERM family of F-actin-associated proteins that is phosphorylated in response to mediators that elevate cAMP responses in gastric parietal cells (12), contains an amphipathic α-helix that binds R_{II} (13). AKAP100, which is enriched in cardiac and skeletal muscle (14), localizes the type II protein kinase A to the sarcoplasmic reticulum and is hypothesized to play a role in the regulation of membrane channel activity. Similarly, protein kinase A anchoring to the postsynaptic densities (15) by AKAP79 is required for modulation of

* This work was supported by National Institutes of Health (NIH) Grants DK48370 and DK43405 (to J. R. G.), a Department of Veterans Affairs Merit Award (to J. R. G.), NIH Grant DK50744 (to S. L. M.), Cystic Fibrosis Foundation Grant MILGR9710 (to S. L. M.), a grant from the National Cancer Institute of Canada with funds from the Canadian Cancer Society (to R. G. H.), a Career Development Fellowship Award from the Canadian Red Cross Society (to J. O. C.), and the Edward Christie Stevens Fellowship from the Faculty of Medicine, University of Toronto (to J. O. C.). The costs of publication of this article were defrayed in part by the payment of page charges. This article must therefore be hereby marked "*advertisement*" in accordance with 18 U.S.C. Section 1734 solely to indicate this fact.

The nucleotide sequence(s) reported in this paper has been submitted to the GenBank™/EBI Data Bank with accession number(s) U26360 (rabbit AKAP350), AF083037 (human gastric AKAP350), AF091711 (human lung AKAP350), and AA471131 (PMY2245).

‡‡ To whom correspondence should be addressed: Institute of Molecular Medicine and Genetics, CB2803 Medical College of Georgia, 1120 15th St., Augusta, GA 30912-3175. Tel.: 706-721-0693; Fax: 706-721-7915; E-mail: jgolden@mail.mcg.edu.

[1] The abbreviations used are: AKAP, protein kinase A-anchoring protein; HGAKAP30, human gastric AKAP350; HLAKAP350, human lung AKAP350; BAC, bacterial artificial chromosome; MDCK, Madin-Darby canine kidney; RACE, rapid amplification of cDNA ends; nt, nucleotide(s); PBS, phosphate-buffered saline; Pipes, 1,4-piperazinediethanesulfonic acid; kb, kilobase pair(s); EGFP, enhanced green fluorescent protein; NMDA, *N*-methyl-D-aspartate.

This is an Open Access article under the CC BY license.

AMPA-kainate currents in hippocampal neurons (16). AKAP15 targets type II protein kinase A to L-type calcium channels in transverse tubules of skeletal muscle and influences rapid voltage-dependent potentiation (17). MAP-2 binds type II protein kinase A and sequesters it in association with dendritic microtubules (4). Phosphorylation of MAP-2 by protein kinase A inhibits microtubule nucleation *in vitro* (3). The distribution of all of these AKAPs suggests that specific scaffolding functions can account for subcellular signaling specificity.

We have previously reported the cloning and initial characterization of a protein kinase A-anchoring protein, AKAP120, from a rabbit gastric parietal cell cDNA library (18). It is now apparent that the initial AKAP120 sequence is a fragment of a larger 350-kDa AKAP (AKAP350). We have completed the sequence of human AKAP350, which represents a multiply spliced family of proteins coded for by a single gene sequence on human chromosome 7q21. Immunolocalization demonstrates that AKAP350 is associated with centrosomes in many cells and also shows noncentrosomal organization in certain epithelial cells, including gastric parietal cells.

EXPERIMENTAL PROCEDURES

Materials—Recombinant R_{II} was purified from bacteria expressing the protein based on a pET11D-R_{II} expression vector (a gift of Dr. John Scott, Vollum Institute). A human tracheal epithelia-enriched LambdaZap cDNA library was a gift from Drs. S. Gabriel and D. Fenstermacher (University of North Carolina, Chapel Hill). Cultured CalU3 and HBE16Eo cells were a gift of Dr. J. Stutts (University of North Carolina, Chapel Hill). Polyclonal anti-γ-tubulin antibody was purchased from Babco (Berkeley, CA). Monoclonal anti-γ-tubulin was purchased from Sigma. Cy2-, Cy3-, and Cy5-conjugated secondary antibodies were purchased from Jackson ImmunoResearch Labs (West Grove, PA). Effectene transfection reagent was obtained from Qiagen (Valencia, CA). Prolong Antifade, 4′,6-diamidino-2-phenylindole, and Alexa 488-conjugated secondary antibodies were from Molecular Probes, Inc. (Eugene, OR). E-GFP-C2 vector, Advantage *Taq*, and Marathon cloning kits were purchased from CLONTECH. All DNA sequencing was performed using dye terminator chemistry automated sequencing in the Molecular Biology Core Facility at the Medical College of Georgia or the DNA Sequencing Facility, University of North Carolina. Oligonucleotides were also synthesized by the Molecular Biology Core Facility. [α-^{32}P]dCTP was purchased from NEN Life Science Products. Random priming kits were purchased from Amersham Pharmacia Biotech. HCT116 cells were obtained from ATCC.

Monoclonal Antibody Production—Recombinant polyhistidine-tagged AKAP120-(183–1022) was prepared by the methods of Dransfield *et al.* (18). Recombinant protein was used to immunize mice, and serum titers were monitored by enzyme-linked immunosorbent assay using the recombinant protein (19). Splenocytes were harvested and fused with myeloma cells. Culture supernatants from the resulting hybridomas were screened by enzyme-linked immunosorbent assay, and productive cell wells were cloned to monoclonal lines by serial dilutional screening. Four monoclonal antibodies were prepared that also detected protein in Western blots. The 14G2 monoclonal antibody, an IgG_1, was used for the present studies because of its detection sensitivity. Monoclonal antibodies were concentrated by preparation of purified IgG from culture supernatants (University of Georgia Monoclonal Facility, Athens, GA).

EGFP-AKAP120—Full-length AKAP120 nucleotide sequence previously cloned into pBluescript (18) was excised with an *Eco*RI restriction digest and ligated in-frame into the pEGFP-C2 vector (CLONTECH). 100 ng of plasmid DNA was transiently transfected into MDCK cells (35-mm dishes) with the Effectene reagent (Qiagen) according to the manufacturer's instructions (20). Cells were grown to confluency and lysed with 1% SDS stop solution.

Western Blot Analysis—Sample extracts from cells and tissues were resolved by SDS-PAGE (3–10% gradient gels) and transferred for 2 h at 750 mA to nitrocellulose (0.22 μm) for subsequent Western blotting. Nitrocellulose blots were blocked with 5% nonfat dry milk in 25 mM Tris-HCl, pH 7.5, 150 mM NaCl for 16–24 h at 4 °C. Blots were then probed in 0.5% nonfat dry milk in 25 mM Tris-HCl, pH 7.5, 150 mM NaCl for 1 h at room temperature with a monoclonal antibody against AKAP350 (14G2; 1:500). After the primary incubation, the blots were washed three times for 15 min each with 25 mM Tris-HCl, pH 7.5, 150 mM NaCl and then incubated with horseradish peroxidase-conjugated anti-mouse IgG (1:2500) for 1 h at room temperature. The blots were finally washed three times for 15 min each with 25 mM Tris/HCl, pH 7.5, 150 mM NaCl, and immunoreactivity was detected with chemiluminescence (Renaissance; NEN Life Science Products) and autoradiography.

Cloning and Sequencing of AKAP350—Both 3′- and 5′-rapid amplification of cDNA ends (RACE) were used to clone the human gastric AKAP350 beginning with sequence information from the human genomic BAC AA004013, which showed homologies with the original AKAP120 sequence. A single 3′-RACE and multiple rounds of 5′-RACE were performed with the Marathon system (CLONTECH) to complete the recloning of human AKAP350 from an end-adapted human gastric cDNA (Marathon cDNA, CLONTECH). Similarly, a rabbit parietal cell cDNA with Marathon adapters was constructed from poly(A) mRNA from a greater than 95% pure rabbit parietal cell preparation. All RACE products were cloned into pBluescript-T (21). Further human sequence information was obtained from the total sequencing of an expressed sequence-tagged cDNA from the human promyeloblast cell line KG1a, PMY2245 (22). Finally, biotinylated recombinant R_{II} was used to screen a human tracheal cDNA library in LambdaZap using a standard protein overlay technique. Phage plaques were identified by incubation in streptavidin-alkaline phosphatase followed by colorimetric detection with a nitro blue tetrazolium/5-bromo-4-chloro-3-indolyl phosphate substrate. Clones were rescued into pBluescript and sequenced. One clone showed homology with rabbit AKAP120 and was sequenced completely.

Northern Blot Analysis—Total rabbit RNAs were prepared from >95% pure parietal cells, gastric fundic mucosa, and lung (23). mRNA was resolved on 1% agarose/formaldehyde gels and transferred to Magnagraph (MSI, Westboro, MA). A human multitissue Northern blot was purchased from CLONTECH. Rabbit blots were probed with a 1650-nt probe corresponding to the 3′-end of rabbit AKAP350 labeled by random priming in the presence of [α-^{32}P]dCTP. Human blots were probed with both a 1650-nt probe corresponding to the 3′-end of human gastric AKAP350 or a 1600-nt probe corresponding to the 5′-end of human lung AKAP350. Blots were probed overnight at 42 °C and then washed to high stringency (0.1× SSC, 65 °C). Dried blots were exposed to either x-ray film at −70 °C or PhosphorImager screens for 72 h.

Splice Variant Analysis—Total RNAs were prepared from tissues and cells using RNASTAT-60 (23). The Advantage RT for PCR kit (CLONTECH) was used to construct cDNA from 2 μg of total RNA using random hexamer primers. Rabbit cDNAs were constructed for parietal cell, spleen, liver, kidney, lung, heart, forebrain, hind brain, and cerebellum and for mucosa from fundus, antrum, duodenum, jejuneum, ileum, and colon. Human cDNAs were also prepared from total RNA obtained from stomach, lung, and kidney, as well as the CalU3 and HBE16Eo cell lines. Gene-specific primers were constructed immediately upstream and downstream from the splice 1 exon (sense, GAACAGTTGGAAGATATGAGACAGGAAC; antisense, GATGCCTCTGCTTCTGACCTCCA), and products were amplified using Advantage Polymerase (CLONTECH) with 40 cycles: 95 °C for 15 s, 60 °C for 10 s, and 68 °C for 60 s. Amplified products were separated on 2% Nuseive 3:1 agarose gels. To amplify the alternative 3′-end coding sequences (splice 2) in human samples, a common sense primer (GGTCGGCCGTCAGAGTATCC) paired with antisense primers specific for either the gastric sequence (AGGATTATCTTCTCATGCCAGCA) or the sequence derived from human lung (ATCCTAATGAGTGTGAAAGAATT) were employed using the same amplification protocol described above. The identities of amplified products were confirmed by gel isolation and DNA sequencing.

Immuncytochemistry in Rabbit Tissues—For investigation of tissue distribution, under anesthesia New Zealand White rabbits were canulated through the distal aorta and perfused sequentially with phosphate-buffered saline (PBS) followed by 4% paraformaldehyde in phosphate buffer, pH 7.4. Tissues were excised and post-fixed for 2 h in 4% paraformaldehyde and then infiltrated with sucrose and embedded in OCT medium. Five-μm frozen sections were cut and mounted on gelatin-coated slides. For staining of gastric glands, isolated gastric glands were prepared from New Zealand White rabbits as described previously (24). Glands were fixed in 4% paraformaldehyde for 30 min at 4 °C, washed in cold PBS, and then permeabilized with 0.3% Triton X-100 in PBS. Glands were then adhered to polylysine-coated slides.

For staining glands and frozen tissue sections, slides were blocked with 17% donkey serum for 30 min and then incubated with 14G2 monoclonal antibody (1:50) or a class-matched nonspecific monoclonal IgG (Sigma) for 2 h at room temperature or overnight at 4 °C. Following washing, antibody localization was detected with incubation with Cy3-

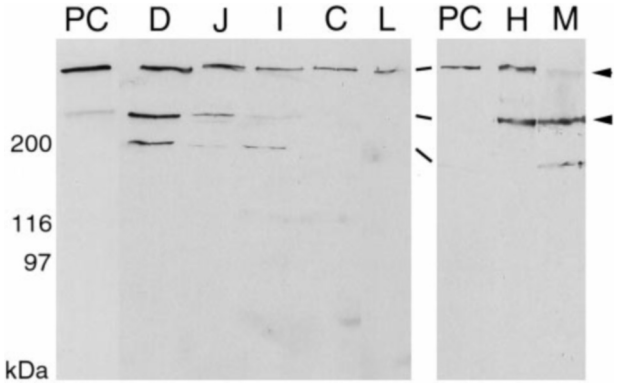

FIG. 1. **Immunoreactivity with 14G2 monoclonal antibody.** Western blots demonstrated a 350-kDa immunoreactive band (*upper arrow*), as well as the intermittently detected 250- (*lower arrow*) and 200-kDa bands in protein extracts (50 μg/lane). *Left*, immunoreactivity was compared between isolated rabbit parietal cells (*PC*) and the following rabbit gastrointestinal tissues: duodenum (*D*), jejunum (*J*), ileum (*I*), colon (*C*), and liver (*L*). *Right*, comparison of rabbit parietal cells with lysates from HeLa cells (*H*) and MDCK (*M*) cells.

donkey anti-mouse IgG antibodies for 30 min at room temperature. Slides were mounted with Prolong Antifade solution (Molecular Probes). Tissue sections were examined under a Zeiss Axiphot microscope equipped with a Sensys digital camera (Photometrics). Gastric glands were examined with confocal fluorescence microscopy (Molecular Dynamics, IMMAG Imaging Core Facility) using maximum intensity projections assembled from 40 0.29-μm optical sections.

Immunocytochemistry in Cultured Cells—HCT116 colon adenocarcinoma cells were plated sparsely on number 1 glass coverslips for 24 h. Cells were washed in PBS and briefly permeabilized in 1% Triton X-100, 45 mM Pipes, 45 mM Hepes, pH 6.9, 10 mM EGTA, 5 mM $MgCl_2$, 0.5 mM AEBSF for 60 s at 4 °C followed by fixation in −20 °C methanol for 6 min. Cells were blocked with 17% donkey serum, 0.1% Tween 20 in PBS and then incubated simultaneously with 14G2 (1:30) and rabbit anti-γ-tubulin (1:400) for 2 h at room temperature. The cells were then simultaneously incubated with ALEXA-488-conjugated anti-mouse IgG and Cy5-conjugated anti-rabbit IgG for 60 min. Following washing in PBS, the cells were incubated in 4′,6-diamidino-2-phenylindole (1 mM) for 5 min and washed in PBS. Coverslips were inverted and mounted with Prolong Antifade. Cells were examined for triple labeling on an Axiophot microscope as described above.

For immunolocalization in MDCK cells, MDCK (type II) cells were grown on 23-mm Transwell clear filters for 3 days to establish highly polarized monolayers. HBE cells were cultured on Transwell filters for 3 days. Cells were then fixed as above for HCT116 cells. Cells were permeabilized and blocked in 10% donkey serum and then incubated with the following primary antibody: 14G2 monoclonal antibodies (1:30); polyclonal rabbit anti-R_{II} (1:1000); rat monoclonal anti-ZO-1 (1:100, a tight junction marker); rabbit anti-γ-tubulin (1:400); or murine anti-γ-tubulin (1:250). Antibodies were visualized with secondary antibodies conjugated with Cy2, Cy3, and Cy5. Immunostained cells were examined by confocal microscopy using maximum intensity projections of 40 0.29-μm optical sections.

Parietal Cell Preparations—Isolated gastric glands and isolated parietal cells were prepared from New Zealand White rabbits as described previously (25). Subfractions of gastric parietal cells were prepared by sequential centrifugation of homogenates at 1000, 4000, 15,000, and 100,000 × *g* to prepare four microsomal pellets and a final high speed supernatant fraction (26). Parietal cells were maintained in primary culture on Matrigel-coated coverslips, as described previously (27). For immunocytochemistry, cultured cells were fixed as for HCT116 cells. Cells were dual-stained as described above with 14G2 and polyclonal anti-γ-tubulin.

RESULTS

Identification of Endogenous AKAP120 Immunoreactivity—Recombinant polyhistidine-tagged AKAP120-(183–1022) was used to make a monoclonal antibodies against the AKAP. Western blots of rabbit parietal cell cytosolic proteins probed with the monoclonal antibody for AKAP120 (14G2) revealed a major band at 350 kDa and a variably detected 250-kDa band (Fig. 1). A 200-kDa band was also intermittently noted. In parietal cells, the variable observation of the 200- and 250-kDa immunoreactive bands in multiple preparations has suggested that they are proteolytic breakdown products. In preparations of protein from rabbit parietal cell subfractions, more than 85% of the total AKAP350 was found in the high speed supernatant (data not shown). A similar banding pattern was seen in a survey of other rabbit tissues by Western blots of protein from duodenum, jejunum, ileum, colon, and liver (Fig. 1). While the most prominent immunoreactive species in all rabbit tissues was a 350-kDa band, 250- and 200-kDa species were also observed. Western blots of cultured epithelial cell lysates also were examined, including nonpolarized HeLa cells and polarized MDCK cells (Fig. 1). Both cultured cell lines demonstrated the 350- and 250-kDa immunoreactive bands. In the MDCK cells, the 250-kDa species was consistently more prominent, although the ratio between the 250- and 350-kDa bands varied considerably.

Although AKAPs tend to migrate in acrylamide gel electrophoresis to higher than predicted molecular weights (8), in light of the Western blots, it was necessary to investigate the possibility that the full-length sequence of the AKAP had not been cloned. A single experiment provided the necessary evidence that the sequence was incomplete. The known AKAP120 sequence was cloned into the pEGFP-C2 vector and transiently transfected into MDCK cells. Duplicate Western blots of cell lysates were then probed with anti-AKAP120 (14G2) and anti-EGFP antibodies. The 14G2 antibody recognized the endogenous 250- and 350-kDa bands as well as a 150-kDa band; however, only the 150-kDa band was seen when probing with anti-EGFP (data not shown). This result indicated that AKAP120 cDNA sequence could not account for endogenous immunoreactive proteins, and therefore the full-length sequence had not been cloned.

Cloning of AKAP350—We sought to complete the cloning from rabbit parietal cells and human gastric cDNAs. Both 3′- and 5′-RACE were used to identify the remainder of the nucleotide sequence. Because a human genomic DNA sequence from chromosome 7q21 corresponding to AKAP120 became available at the time, we chose to focus on the human clone. This has led to the cloning of the full-length human sequence composed of 11,490 base pairs with an open reading frame of 10,593 nucleotides (Fig. 2). The 5′-end of the sequence contains a strong consensus initiation sequence, which is preceded by two upstream in-frame stop codons. From the first in-frame ATG, this sequence codes for 3531 amino acids with a predicted molecular mass of 409 kDa and a pI of 4.8. Because of its migration in SDS-PAGE, we have named this new full-length sequence AKAP350. The sequence contains 58 phosphorylation sites for protein kinase C, 56 for casein kinase II, and three for tyrosine kinase. protein kinase A phosphorylation sites are predicted at residues 1860, 2285, 2727, and 3076. An R_{II} binding region previously identified in the AKAP120 sequence is found from amino acid 2174 to 2187 in the human AKAP350 (Fig. 2). These sites are identical except for a single isoleucine to valine substitution, which should not affect the integrity of the amphipathic helix. Four leucine zipper motifs are present between amino acids 313 and 334, 391 and 412, 2651 and 2672, and 3211 and 3239 (Fig. 2).

A closer examination of the peptide sequence for AKAP350 reveals a structure involving multiple coiled-coil domains throughout the protein, especially from amino acid 739 to 2270. The AKAP350 protein is 15.3% glutamate, 9.3% glutamine, and 12.4% leucine by total amino acid composition. In 62 individual locations, two consecutive glutamate residues are found, and in 21 locations, two consecutive glutamine resi-

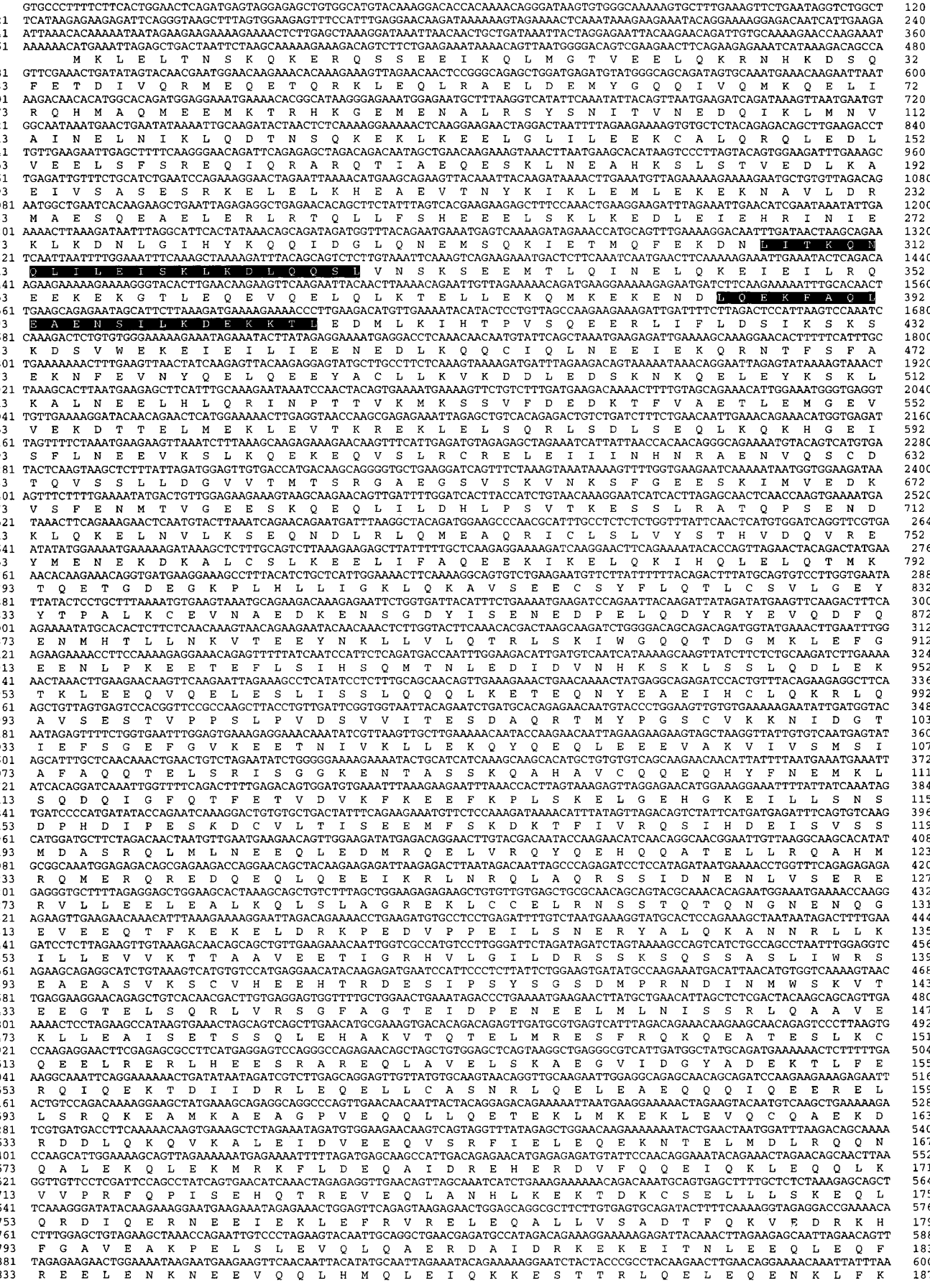

FIG. 2. **Alignment of full nucleotide and amino acid sequence for human gastric AKAP350.** The positions of the R_{II} binding site (*underlined*) and the four leucine zippers (*highlighted*) are noted.

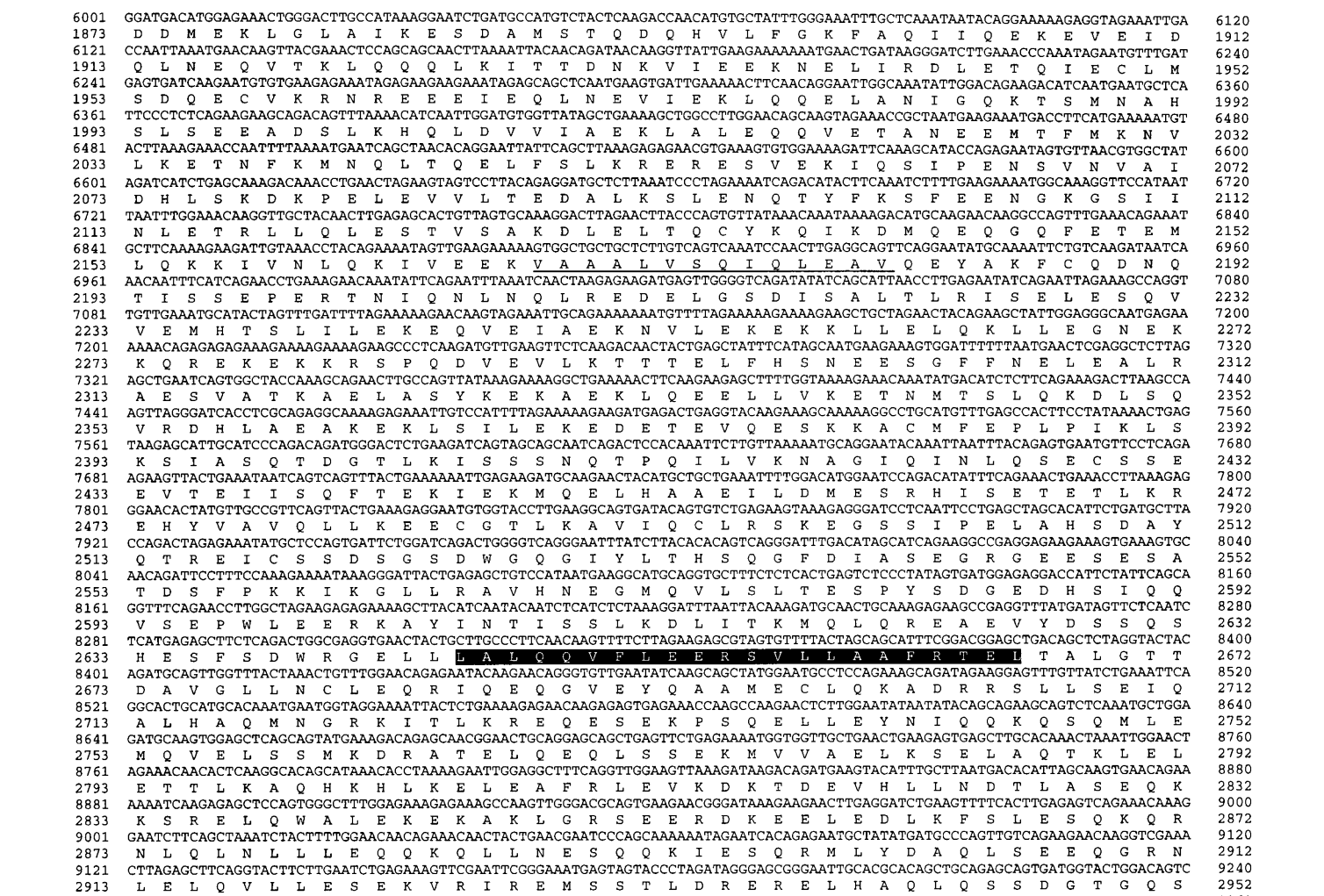

FIG. 2—*continued*

dues are found.

By conducting searches of on-line data bases including Fasta, PROSITE, and BLAST, other proteins possessing significant homology with the human AKAP350 were identified. The original rabbit parietal cell AKAP120 protein sequence is 78% identical to the human gastric AKAP350 (HGAKAP350) sequence. Yotiao, a recently described ligand of the NR-1 subunit of the NMDA receptor (29) shares the same genomic DNA region as AKAP350. This protein is 99% identical to amino acids 1–1249 (YHR, Fig. 3) of HGAKAP350. The human

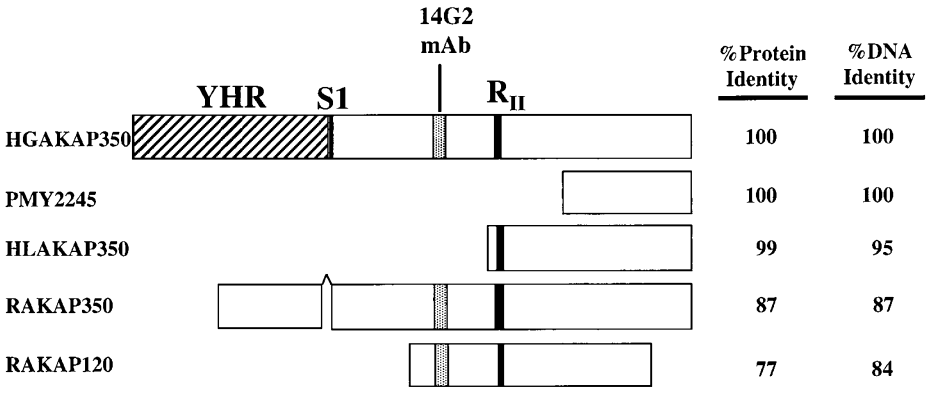

FIG. 3. **Comparison of cDNAs coding for AKAP350.** The HGAKAP350 is compared with the structures of the PMY2245 promyeloblast expressed sequence clone, the HLAKAP350 cDNA, rabbit parietal cell AKAP350 (*RAKAP350*), and the original rabbit AKAP120 sequence (*RAKAP120*). The percentages of protein and DNA sequence identities *versus* HGAKAP350 are shown at the *right*. The HGAKAP350 sequence contained an amino-terminal yotiao homology region (*YHR*) followed immediately by a site of major splice variants (*S1*). The RAKAP350 sequence is missing a single exon at the S1 splice site (see Fig. 5*b*). Note also the region recognized by the 14G2 monoclonal antibody to AKAP350 (amino acids 1478–1547 in RAKAP350 and 1854–1958 in HGAKAP350) and the position of the R_{II} binding site.

AKAP350 cDNA maps onto chromosome 7q21 in the genomic DNA of BACs 4013, 0066, 3086, and 0120 while splicing in and out of yotiao exons. Approximately 50% of the coding sequence for yotiao is found in exons for AKAP350. Another protein with significant homology is pericentrin, a 220-kDa coiled-coil protein found in centrosomes and pericentriolar material. Pericentrin shares a 21% identity and 47% similarity with AKAP350. Other centrosomal associated proteins sharing similarity with AKAP350 include CENP-F (20.7%), and CEP250 (20.2%). Other cytoskeletal proteins with 20–24% identity include two intermediate filament binding proteins, plectin and tricohyalin, as well as a number of other proteins with extensive coiled-coil domains including myosin heavy chain, giantin, and the Golgi antigen GCP372.

Additional sequence for AKAP350 was acquired by examination of other cDNAs obtained from human lung, rabbit parietal cell, and the longest expressed sequence tag with homology to the known AKAP sequence, PMY2245 (Fig. 3). Sequencing of the PMY2245 clone from a human promyeloblast cell line revealed 100% identity to the human gastric AKAP350 (HGAKAP350) over approximately 4 kb of sequence at the 3′-end (Fig. 3). Human lung cDNA yielded a clone (HLAKAP350) with 99% protein identity and 95% DNA identity over a 4-kb segment also at the 3′-end of the AKAP. From rabbit parietal cell cDNA, a partial sequence was obtained from 5′- and 3′-RACE products, accounting for all but the 1000 nt at the 5′-end, 91% of the total human gastric AKAP350, with 87% protein identity and 87% DNA identity to HGAKAP350.

AKAP350 Genomic Structure—A comparison of the resolved cDNA sequences from human stomach, human lung, rabbit parietal cells, and the expressed sequence tag cDNA (PMY2245) with the genomic sequences have allowed us to map the exons of this gene. The AKAP350 exons are scattered over 200 kb of genomic DNA (Fig. 4*a*). This genomic region apparently codes for a multiply spliced gene that includes DNA for the yotiao protein and several forms of AKAP350. Upstream from the first yotiao exon, there is a GC-rich region that probably represents a TATA-less promoter. The first exon of AKAP350 lies between exons 9 and 10 of yotiao. Upstream from the AKAP350 first exon is a promoter region that contains two putative TATA box elements.

At least three major sites of alternate splicing exist in the AKAP350 sequence. The first location is a highly spliced region where three separate splice choices are made including a read-through to complete the final yotiao exon or a choice in AKAP350 of two different splice acceptors for a common splice donor (Fig. 4*b*). The latter splice variant (Fig. 4*b*) was observed in the rabbit parietal cell AKAP350 cDNA sequence, representing the loss of an entire exon immediately following the yotiao homology region. To examine the incidence of this splice variant, this region was amplified from multiple rabbit tissue cDNAs with specific primers (Fig. 5*a*). Most mucosal tissues from rabbit gastrointestinal tract predominantly express the transcript with the S1 region deleted. Overloading of samples reveals that parietal cells and other gastrointestinal mucosae do express a small amount of the larger transcript. In contrast with the mucosal samples, in smooth muscle from the gastric wall the larger splice variant predominates. Other rabbit tissues such as heart and brain reveal the presence of the larger variant exclusively. The third (highest) band observed in forebrain, hind brain, and cerebellum was sequenced and found to be an artifactual amplification of phosphofructokinase.

Alternative splicing also was found at the C terminus of the protein (Fig. 4*c*). While the human gastric, rabbit parietal cell, and promyeloblast cDNAs all showed the same 3′ sequences, the cDNA obtained from the tracheal cDNA library (HLAKAP350) demonstrated a different 3′ sequence resulting from a read-through extending past the splice donor site (similar to that seen for the final yotiao exon). This "missed splice" allows the cDNA sequence to continue for another 435 base pairs before terminating. The incidence of these variants was again surveyed using locus-specific primers and amplification from cDNA of several human tissues and the Calu-3 and HBE cultured cell lines (Fig. 5*b*). Both splice variants were observed in pancreas, gastric and lung cDNAs (Fig. 5*b*). However, the 497-base pair product, which is characteristic of the cDNA derived from the human tracheal cDNA, was not observed in either Calu-3 or HBE cells. Only the 397-base pair product was observed in these cell lines.

Finally, comparison of the PMY2245 cDNA from promyeloblasts with the sequences from human lung and human stomach showed a loss of 8 amino acids (24 nt). Examination of the genomic sequence showed that a variation in the choice of splice donor sites accounted for this small sequence deletion. There are also several instances in the rabbit AKAP350 sequence where 1–3 amino acids have been lost or gained. Because the rabbit genomic sequence is not available, we cannot presently evaluate whether these differences are due to splice variation or interspecies variations.

Northern Blot Analysis of AKAP350 Expression—Northern blotting with the 3′ end of HGAKAP350 as a probe, revealed an 11-kb message found in rabbit parietal cells and rabbit fundus,

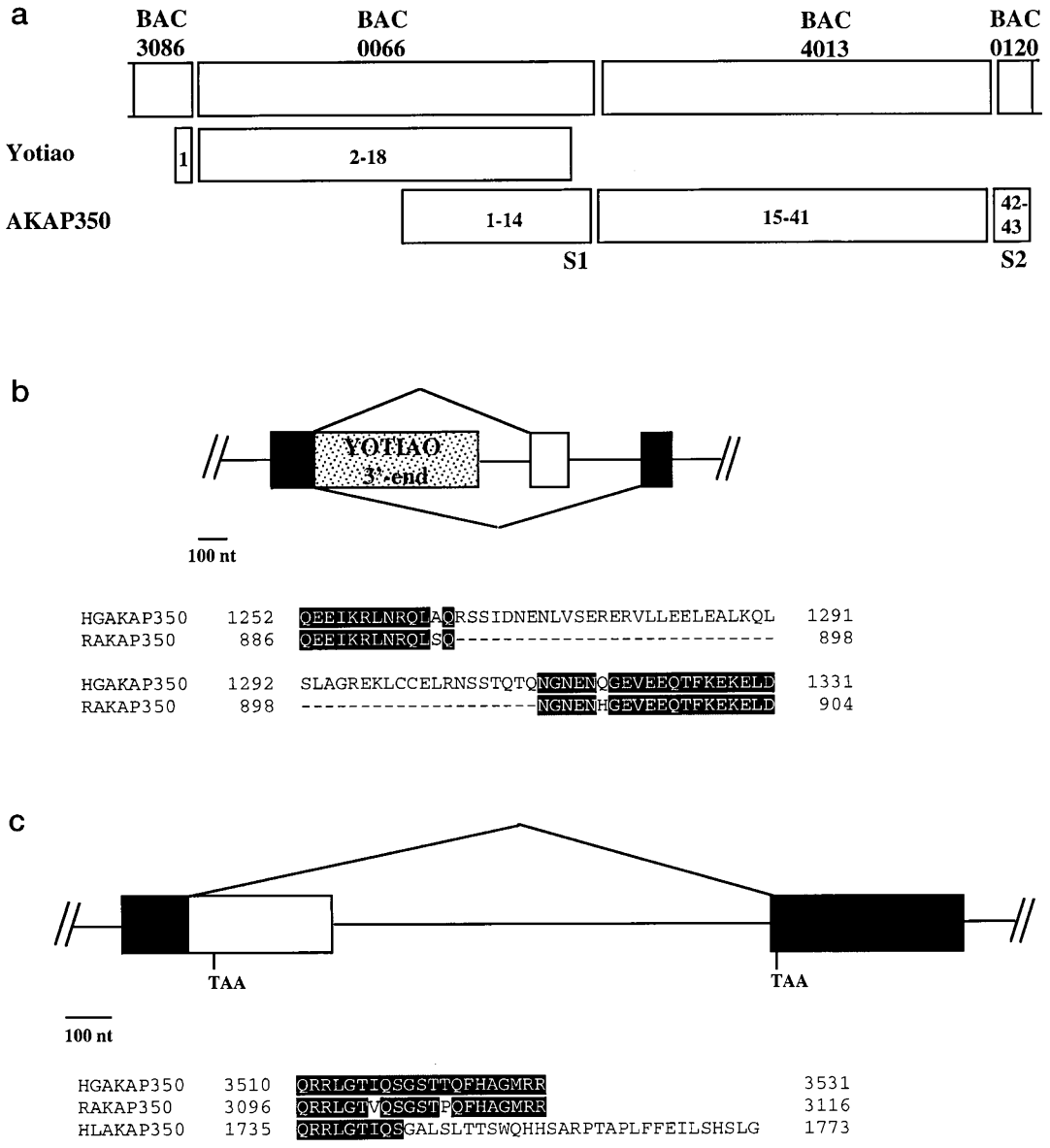

FIG. 4. **Multiple splicing in AKAP350.** *a*, exons composing the DNA sequence for both yotiao and AKAP350 are labeled according to the BAC in which they are found. *S1* and *S2* denote the sites of alternative splicing to generate isoforms. Note that the *figure* shows BAC AA000066 in the reverse orientation to its numbering in its GenBank™ entry. *b*, map of the S1 splice region and corresponding amino acid sequence. The *shaded region* codes for the terminal 3′ end of yotiao. A splice before this sequence to the next exon occurs in human gastric AKAP350, whereas in rabbit AKAP350 this exon is spliced out. *c*, map of S2 splice region and corresponding amino acid sequence. The 3′ end of both human and rabbit AKAP350 splice into the last exon at a point read through by the AKAP350 sequence in human lung. The HLAKAP350 therefore contains 18 additional amino aicds, resulting in a larger 3′-end in this isoform.

as well as in rabbit lung (Fig. 6). Human multitissue Northern blots probed with either a 1.6-kb fragment from the 5′-end of HLAKAP350 (Fig. 6) or a 1.0-kb fragment of the 3′-end of rabbit parietal cell AKAP350 (data not shown) demonstrated two bands, 9.5 and 11 kb, most prominent in kidney and skeletal muscle and to a lesser extent in lung. Only the 9.5-kb message was noted in liver, and only the 11-kb message was observed in heart and brain.

AKAP350 Localization in Rabbit Tissues—To investigate the subcellular localization of AKAP350, the 14G2 monoclonal antibody was used to stain rabbit tissue sections and isolated gastric glands. In the gastric fundus, parietal cells demonstrated multiple foci of immunostaining throughout the cytosol (Fig. 7*a*). Confocal fluorescence microscopic examination of isolated gastric glands also demonstrated multiple foci of staining in parietal cells (Fig. 7*b*). This immunostaining in parietal cells did not coincide with staining for either the H/K-ATPase-containing tubulovesicles or F-actin-staining secretory canalicular membranes (data not shown). In the esophagus, basal cells appeared to show a single point of bright fluorescence (Fig. 7*c*). In the jejunum, the most prominent staining was observed in submucosal lymphoblasts, which showed a single focus of perinuclear staining (Fig. 7*d*). In the ileum and colon, epithelial cells of the deep crypts were strongly stained with multiple bright foci just beneath the apical membranes (Fig. 7, *e* and *f*). In pancreatic islets, strong AKAP350 immunostaining was present in all of the endocrine cells of the islet (Fig. 7*g*). In many cells, multiple foci of staining were apparent in the perinuclear region. In contrast, adrenal medullary cells demonstrated only a single focus of AKAP350 immunostaining in all cells (Fig. 7*h*). In the kidney collecting duct, AKAP350 staining was observed as a single focus of staining deep to the apical membrane (Fig. 7*i*). Single foci of immunostaining also were observed in primary and secondary germ cells in the

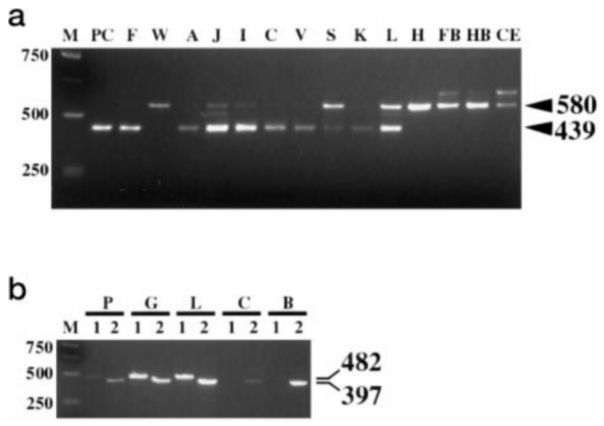

FIG. 5. **Tissue survey for splice variants by the polymerase chain reaction method.** *a*, the S1 region in Fig. 4 was amplified in an array of rabbit tissues including parietal cells (*PC*), fundus (*F*), gastric wall smooth muscle (*G*), antrum (*A*), jejunum (*J*), ileum (*I*), colon (*C*), liver (*V*), spleen (*S*), kidney (*K*), lung (*L*), heart (*H*), forebrain (*FB*), hind brain (*HB*), cerebellum (*CE*). *b*, The S2 region in Fig. 4 was amplified from cDNA from human pancreas (*P*), stomach (*G*), lung (*L*), Calu-3 cells (*C*), and human bronchial epithelium (*B*). For each cDNA, two reactions were performed: one with an antisense primer specific for the longer 3′ end splice variant (*1*) and a second time with an antisense primer specific for the shorter splice (*2*).

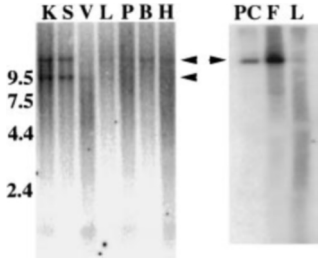

FIG. 6. **Northern blots of AKAP350 mRNA expression.** Rabbit (*right*) tissues were probed with the 3′-end of HGAKAP350, revealing an 11-kb message for rabbit parietal cell (*PC*), fundus (*F*), and lung (*L*). Human tissue, including kidney (*K*), skeletal muscle (*S*), liver (*V*), lung (*L*), placenta (*P*), brain (*B*), and heart (*H*), was probed with a 1-kb fragment of HLAKAP350.

testes (Fig. 7*j*). Finally, in the epithelial cells lining the ductus efferens and the bronchial epithelium, mutiple foci of AKAP350 immunostaining were observed deep to the apical membranes (Fig. 7, *k* and *l*).

AKAP350 Is Associated with Centrosomes—The perinuclear localization of AKAP350 in many cells suggested its association with centrosomes. We therefore studied the localization of AKAP350 in HCT116, a moderately differentiated colonic adenocarcinoma cell line. In interphase cells, AKAP350 immunostaining colocalized with γ-tubulin staining (Fig. 8). During metaphase, AKAP350 immunostaining was concentrated in both centrosomes colabeling with γ-tubulin. However, in both anaphase and telophase cells, while AKAP350 immunostaining colocalized with γ-tubulin-staining centrosomes, several discrete foci of staining also were present in the cleavage furrow of dividing cells. An identical distribution during the cell cycle was also observed in HeLa cells (data not shown). These results indicate that AKAP350 is associated with centrosomes in rapidly dividing cells.

Since HCT116 cells are not polarized, we also sought to investigate AKAP350 distribution in polarized cells. MDCK cells, a well established polarized kidney cell line, were grown on permeable filters. While multiple foci of immunostaining for R_{II} were present throughout the cytosol, AKAP350 staining was only present in one focus per cell colabeling with major points of R_{II} staining (Fig. 9*b*). Colabeling of MDCK cells for AKAP350 and γ-tubulin showed clear colocalization at the centrosomes; however, there was obvious asymmetry between the poles. Higher resolution projections demonstrate that AKAP350 staining predominates in one centriole as a projection radiating toward the nucleus. Examination of centrosomal staining with R_{II} antibodies (Fig. 9, *m–o*) showed a similar R_{II} immunostaining projection from one pole of the γ-tubulin-staining centrosome. Treatment of MDCK cells with nocodazole (33 μM) to disrupt microtubules did not alter the association of either AKAP350 or R_{II} with the centrosomes (data not shown).

Finally, since several rabbit cells including gastric parietal cells and bronchial epithelium showed multiple foci of AKAP350 staining, we also examined in greater detail AKAP350 staining in primary cultures of rabbit parietal cells and human bronchial epithelial cells. In parietal cells, multiple foci of AKAP350 staining were observed throughout the cell (Fig. 10). One perinuclear focus coincided with staining by antibodies against γ-tubulin, but the vast majority of AKAP350 foci did not correspond with the centrosomes. AKAP350 foci also did not coincide with F-actin staining of the intracellular canaliculus (data not shown). In human airway epithelial cells, the major staining was associated with centrosomes; however, prominent staining of foci associated with the lateral aspects of the subapical regions also were present. A similar pattern of noncentrosomal staining was observed in T84 and HCA-7 colon adenocarcinoma cells (data not shown).

DISCUSSION

Protein kinase A-anchoring proteins represent a diverse superfamily of scaffolding proteins. This report clarifies the characteristics of a novel multiply spliced AKAP family. Monoclonal antibodies raised against AKAP120 identified proteins of 350 and 250 kDa in most tissues and cells. AKAP120 was originally cloned from a rabbit parietal cell cDNA expression library using ^{32}P-labeled R_{II} as a probe. The single clone isolated yielded an open reading frame of 3500-nt cDNA coding for a recombinant expressed protein migrating with an apparent molecular mass of 120 kDa (18). As described above, eukaryotic expression of this AKAP sequence as a fusion with the EGFP indicated that the AKAP120 clone could not account for the endogenous 350-kDa immunoreactive species. The results of our cloning experiments reported here show that the original clone was not full-length and included an erroneous stop codon. The full-length sequence of AKAP350 contains at least two major areas for alternative splicing. In addition, genomic sequence also contains a major spliced product that codes for the previously described yotiao protein (29). The present sequence length matches the major mRNA length observed in rabbit and human tissues of over 11 kb. Our results demonstrate that splice variants may be differentially distributed among tissue and cell types. Indeed, since smaller 9.5-kb species of mRNA have been identified in Northern blots, it is possible that further splice variants may be present.

Previously, a multiply spliced murine AKAP gene has been described, yielding six isoforms, collectively known as AKAP-KL (30). Parallel cloning of the AKAP350 in both rabbit and human has revealed multiple splice variants. Additionally, the existence of the yotiao protein coding region as a 5′-end splice variant indicates that the AKAP350 genomic region produces a complex family of protein products from internal alternative exon splicing as well as alternative splicing at both the 5′- and 3′-ends. The function of specific spliced exons remains to be determined. It is tempting to suggest that specific spliced exons may account for proper targeting of the AKAP or interaction with specific proteins. This possibility appears especially

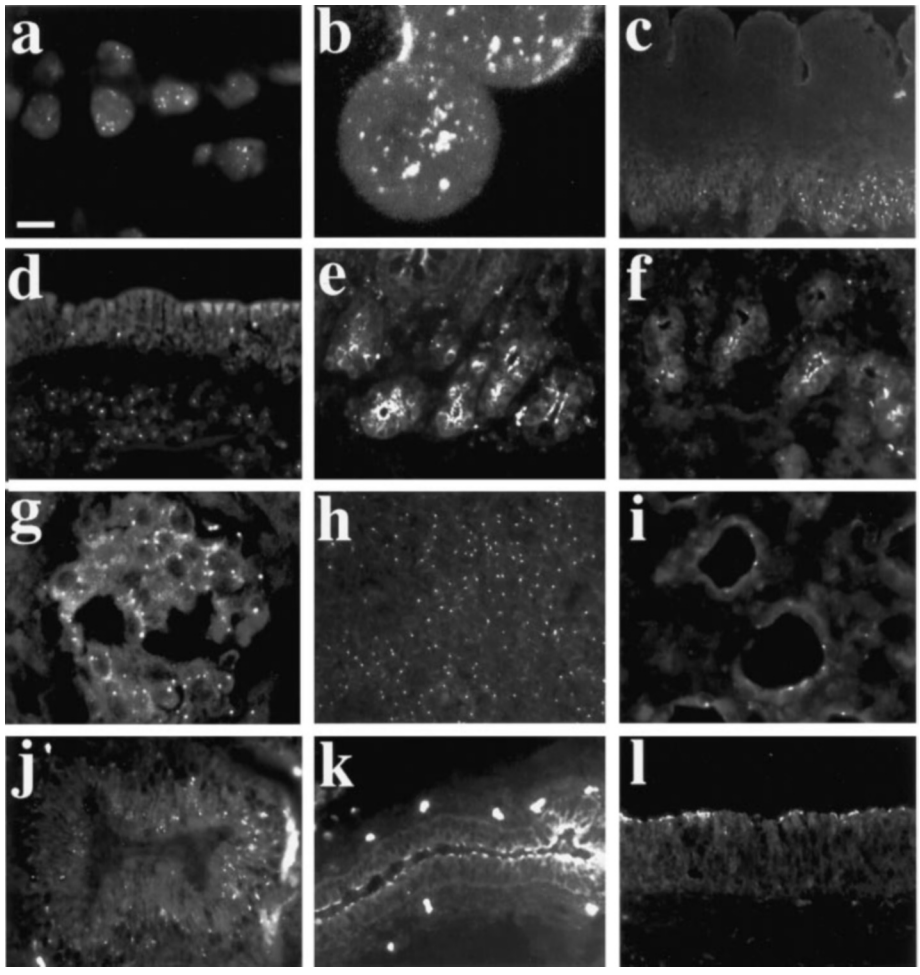

FIG. 7. **Distribution of AKAP350 in rabbit tissues.** The distribution of AKAP350 was examined using the 14G2 monoclonal antibody in tissue sections and isolated gastric glands (*b*). AKAP350 staining was localized in frozen sections of gastric fundic mucosa (*a*), esophagus (*c*), jejunum (*d*), ileum (*e*), colon (*f*), pancreatic islet (*g*), adrenal medulla (*h*), renal collecting duct (*i*), testes (*j*), ductus efferens (*k*), and tracheal epithelium (*l*). Nonspecific staining of large submucosal macrophages in ductus efferens sections was also observed in controls incubated with no primary antibody. Multiple points of AKAP350 immunofluorescence were observed in parietal cells of gastric glands (*b*) visualized through confocal fluorescence microscopy with maximum intensity reconstruction of 40 0.29-μm optical sections. *Bar*, 12 μm (*a*, *g*, *i*, and *l*), 3 μm (*b*), 24 μm (*c*, *d*, *e*, *f*, *h*, *j*, *k*).

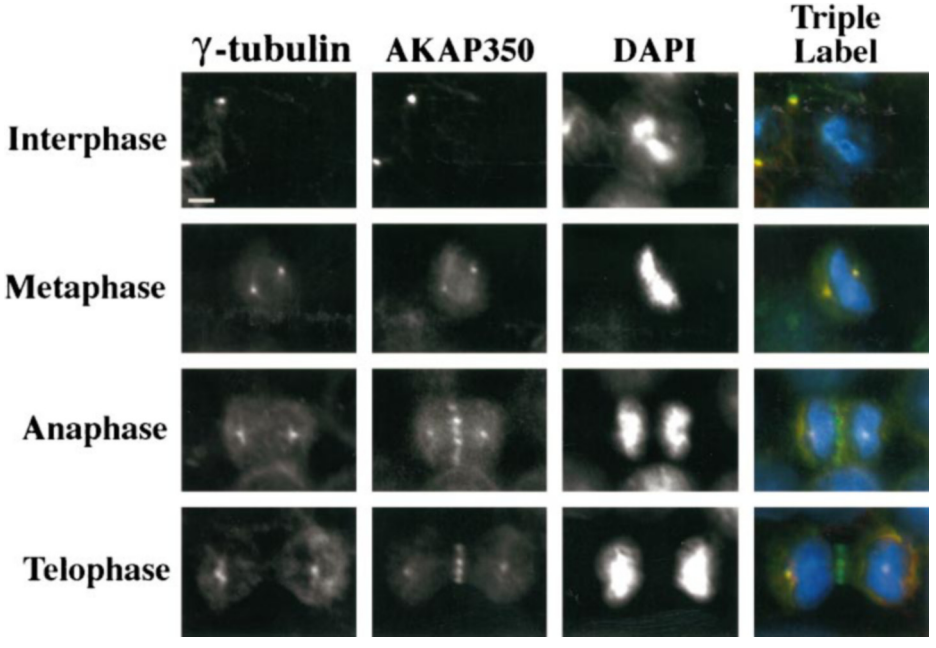

FIG. 8. **Distribution of AKAP350 during mitosis.** HCT116 cells were plated at low density for 24 h and then fixed. Cells were triple labeled with polyclonal anti-γ-tubulin, monoclonal anti-AKAP350 (14G2) and 4′,6-diamidino-2-phenylindole. A triple label overlay of the staining patterns is shown at the *right*. Based on the 4′,6-diamidino-2-phenylindole staining, cells were identified according to their mitotic phase as interphase, metaphase, anaphase, or telophase. At interphase, a single nidus of AKAP350 staining coincided with the γ-tubulin staining adjacent to the nucleus. In metaphase, AKAP350 stained both of the centrosomal poles and, in addition, a diffuse cytosolic staining was also observed. During anaphase and telophase, AKAP350 immunostaining was associated with the centrosomes, but discrete foci of staining were also present in the cleavage furrow. *Bar*, 3 μm.

possible for the highly spliced region within BAC AA0066, which contains the alternate splice point for the terminal exon of yotiao as well as the major internal alternatively spliced exon in AKAP350, immediately following the yotiao homology region. The AKAP350 sequence lacking this exon was the major sequence in rabbit parietal cells as well as in most gastrointestinal mucosae. In contrast, the sequence including this 140-nt sequence was predominant in gastric wall smooth muscle and brain tissue. Interestingly, this exon includes a pair of adjacent cysteines, perhaps indicative of a possible covalent cross-linking point either for homodimerization or interaction with other proteins.

A second major splice variation occurs at the C terminus of AKAP350 as described above. The AKAP350 sequence isolated

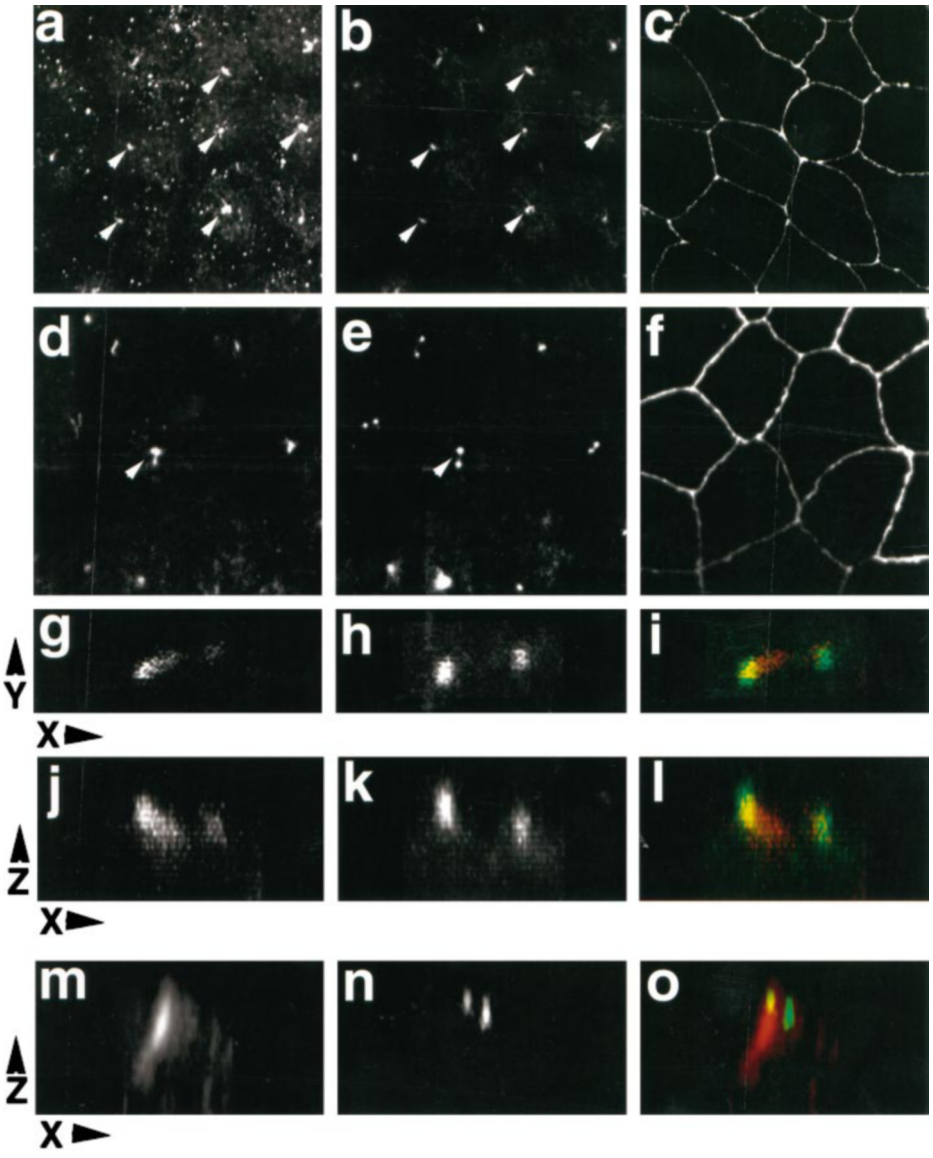

FIG. 9. **Association of AKAP350 with centrosomes in polarized MDCK cells.** MDCK cells were grown on permeable filters for 3 days and then fixed. *a–c*, cells were triple stained with polyclonal anti-R_{II} (*a*), murine monoclonal anti-AKAP350 (14G2) (*b*), and rat monoclonal anti-ZO-1 (tight junctions) (*c*). Cells were imaged as maximum intensity projections of 40 0.29-μm optical sections. The *arrowheads* show regions of colocalization of AKAP350 staining with staining for R_{II}. *d–l*, cells were triple labeled with murine monoclonal anti-AKAP350 (*d*, *g*, *j*), polyclonal anti-γ-tubulin (*e*, *h*, *k*) and rat monoclonal anti-ZO-1 (*f*). AKAP350 labeled the poles of the centrosomes assymetrically (*arrowheads*). Cells were imaged as maximum intensity projections of 40 0.29-μm optical sections. *X-Y* (*g–i*) and *X-Z* (*j–l*) projections of a single pair of centrioles shows that AKAP350 immunoreactivity was concentrated as a projection from one of the centrioles (dual label overlaps in *i* and *l*). The projection always was oriented away from the apical membrane. A similar distribution was observed for R_{II} immunostaining (*m*) in association with γ-tubulin staining centrioles (*n*). The dual label image (*o*) of the *X-Z* reconstruction of a pair of centrioles shows a similar pattern of a projection from one pole of the centriole. *Bar*, 5 μm (*a–c*), 3 μm (*d–f*), 1 μm (*g–o*).

from the tracheal cDNA library results in an alternative 16 carboxyl-terminal amino acids not found in the human gastric or the promyeloblast sequence due to a splice variant in the next to last exon. Since the end of this exon coincides with multiple consecutive adenosines, it is unlikely that this is the true 3′-end in this mRNA. It is more probable that oligo(dT) priming occurred internally at the polyadenine in the mRNA 3′-untranslated region. Analysis of this splice variant has demonstrated its presence in several tissues. However, while both 3′ splice variant sequences were detected in whole lung cDNA, when we examined cDNA from CalU3 cells (a lung serous cell line) and a human bronchial epithelial cell line, we were unable to detect the 3′ splice variant originally isolated from the bronchial epithelial cell library. Since the library was constructed from only an enriched population of tracheal epithelial cells, it seems likely that the message must emanate from a nonepithelial lung cell. These data further suggest that there is a cell-specific distribution of these AKAP350 isoforms. In addition to the two major splice variants, the PMY2245 expressed sequenced tag cDNA also demonstrated a minor splice variant yielding a deletion of eight amino acids (24 nt) because of an alternate splice donor choice. Given the theoretical function of AKAPs, it appears reasonable that these splice variants may define either specific intracellular targeting for particular AKAP350 isoforms in different cell types or their association with specific scaffolding components.

Alternative splicing of this nature has been well characterized in several complex spliced protein families including odorant receptors (31), neurexins (32), and myofibrillar proteins (33). Contractile protein genes provide a model system for study of this process. Either a particular gene among members of a multigene family is selected for expression or a spectrum of different proteins may be generated from a single gene. A prime example of both is found in troponin T, a member of the thin filament of vertebrate sarcomere with specific subtypes in cardiac as well as fast and slow skeletal muscle (Tc, Tf, Ts). Each subtype is coded by a gene with a unique promoter region and terminates at a single polyadenylation site. Within each subtype, however, a series of adjacent exons are intermittently spliced out, forming a large number of isoforms (32 for Tf) coded by the same gene. Gene transcripts are assembled from variations in both donor and acceptor splice site selection (33).

The results of our investigations have shown that AKAP350 and yotiao are products of the same genomic region on chromosome 7q21. Yotiao was identified as a protein in brain that interacts with the NMDA receptor subunit NR1 (29). Interestingly, the regions that mediate this interaction also are present in the amino-terminal region of AKAP350. Examination of the

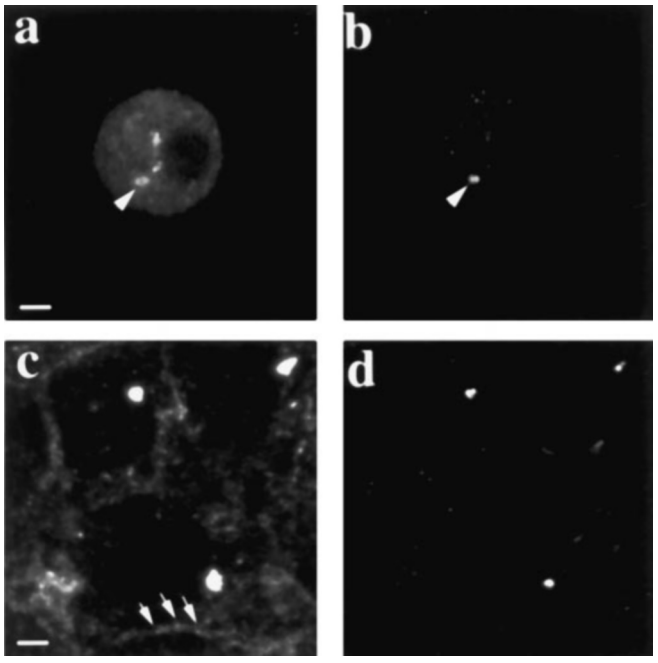

FIG. 10. **Noncentrosomal AKAP350 in cultured cells.** Primary cultures of gastric parietal cells (*a*, *b*) and cultured human bronchial epithelial cells (*c*, *d*) were dual stained with antibodies against AKAP350 (*a*, *c*) and γ-tubulin (*b–d*). Single 0.29-μm optical sections were used to evaluate the distribution of the immunostaining. In parietal cells, while AKAP350 staining could be seen in association with centrosomes (*arrowheads*), the majority of the staining was not associated with γ-tubulin staining. In airway epithelial cells, the majority of AKAP350 staining was associated with centrosomes, but discrete foci of AKAP350 staining were also present in the apical region of the cell, especially near the lateral borders (*arrows*). *Bar*, 3 μm.

genomic sequence region upstream of the yotiao coding region suggests that there is a GC-rich putative promoter region. The genomic region upstream of the 5′-end of the AKAP350 sequence contains a putative TATA box and other putative regulatory elements. Thus, the two proteins probably have separate transcriptional regulators. The 14G2 antibody that we have used in our immunolocalization studies recognizes a region of AKAP350 that is not contained in yotiao. Thus, our localization studies are specific for AKAP350. In contrast, the antibodies used in studies of yotiao are raised against regions that are predicted to cross-react with AKAP350 (29). Indeed, it is interesting to note that the size of the major species observed in whole brain was considerably larger than the size of yotiao protein exogenously expressed in fibroblasts (29). Some of the assignment of yotiao staining and distribution may need to be reevaluated with more specific antisera against the far amino or carboxyl termini of yotiao. In addition, it will be of interest to identify whether AKAP350 in brain also interacts with an NMDA receptor.

An extensive amount of study has been dedicated to elucidating the function of the centrosome and its components as they relate to the general physiology of the cell. The centrosome is the principal microtubule organizing center in most cells, composed of a pair of centrioles and a surrounding matrix, also referred to as the pericentriolar material. Each centriole has bilateral appendages at one pole known as transitional fibers (34). γ-Tubulin is a major component of the centriole cores in a variety of cells (35), and several studies suggest that this protein may be essential for microtubule nucleation from centrosomes (36). As one might expect for an organelle central to cytoskeletal organization, a number of regulatory molecules also are associated with the centrosome. The importance of protein phosphorylation in microtubule nucleation is underscored by the presence of the $p34^{cdc2}$ kinase and type II protein kinase A at the centrosome (7, 8, 37). Keryer *et al.* (9) subsequently studied the distribution of R_{II} isoforms α and β in a human lymphoblast cell line, finding the R_{II}-β localized to the Golgi-centrosomal area. The characteristics of the 350-kDa AKAP that we have cloned appear similar to those of the centrosomal AKAP350 identified by Keryer *et al.* (9) in an R_{II} blot overlay of isolated centrosome proteins from the KE37 human lymphoblast cell line. These investigators immunoprecipitated the protein using the serum 0013 polyclonal antibody, previously reported as a specific marker for human centrosomes (20, 22, 38). No further characterization of this protein in the literature has been submitted, however, since the initial report. Nevertheless, several lines of evidence suggest that this protein may indeed be identical to the protein cloned here. First, Western blots with our 14G2 monoclonal antibody show a similar pattern of 250- and 350-kDa proteins as seen by Keryer *et al.* (9) with the 0013 polyclonal serum and R_{II} overlays. Second, immunocytochemistry with the 14G2 monoclonal antibody also shows prominent localization of the protein with the centrosomes of both polarized and nonpolarized cells. Third, as noted for the AKAP350 protein previously described, the distribution of 14G2 immunoreactive protein in MDCK cells was not altered by treatment of cells with nocodozole.

AKAPs are well characterized as scaffolding proteins, sequestering the R_{II} subunit and consequently the catalytic subunit of the protein kinase A in a location where phosphorylation of a particular substrate will be needed for some key regulatory process (39, 40). Centrosomes, as the site of microtubule nucleation and mitotic spindle formation as well as a binding site for several centrosome-associated proteins, provide a host of possible substrates for regulation by protein kinase A phosphorylation. A role for AKAPs in microtubule nucleation has previously been established in the case of MAP-2 (3). In immunocytochemical analysis, γ-tubulin has become the marker of choice for the centrosomes; however, it is now clear that many cell types also have noncentrosomal pools of γ-tubulin. This does not seem to be the case in the MDCK cell line, where γ-tubulin staining and AKAP350 were limited to the discrete pair of centrioles forming the centrosome. Parietal cells, at the other end of the spectrum, display multiple foci of AKAP350 labeling throughout the cell. These other sites do not correlate with γ-tubulin staining in parietal cells. While most tissues and cells demonstrate AKAP350 distribution in association with centrosomes, several epithelial cells also showed noncentrosomal staining patterns. In the human airway epithelial cell line, for example, the majority of AKAP350 staining appears at the centrosome; however, it is also apparent in a lateral subapical pattern. Similar permutations of AKAP350 distribution in these and other epithelial cells (*e.g.* colonic epithelial cells) allow us to speculate that the protein kinase A is probably targeted to cytoskeletal elements other than centrosomes in many cell types.

Confocal immunofluorescence microscopy demonstrated AKAP350 staining associated with large globular complexes scattered throughout the cytosol of parietal cells, lending support to the idea that this protein is part of a complex of regulatory molecules. The presence of multiple AKAP350-containing structures in parietal cells may reflect its involvement in the massive cytoskeletal reorganization that takes place when parietal cells are stimulated to secrete acid (27). Other less differentiated cell types, especially those that have undergone transformation into a phase of unregulated growth, may require AKAP350 simply for microtubule nucleation at the centrosome; hence, the distribution is strictly limited to this organelle. Examination of the mitotic spindle apparatus in the

stages of mitosis in HeLa and HCT116 colon adenocarcinoma cells demonstrated the presence of AKAP350 not only at the centrosome throughout mitosis but also at the cleavage furrow in anaphase and telophase for both cell types. This finding might suggest a possible role for AKAP350 in establishment or activation of contraction to form the contractile ring in telophase cells. Interestingly, no R_{II} was observed in association with AKAP350 in the cleavage furrow. This may suggest that an alternate splice variant, different from centrosomal AKAP350, is associated with a different cytoskeletal system. Of note, the extensive coiled-coil structure in AKAP350 shows homology not only to centrosome-associated proteins (*e.g.* pericentrin) but also to intermediate filament-associated proteins and myosins. In addition to alternate cytoskeletal association, it is also likely that AKAP350 is scaffolding other regulators beyond type II protein kinase A. Along these lines, AKAP79 is associated with both protein phosphatase and protein kinase C (28). Further investigations will be required to elucidate components of the AKAP350 scaffolding complex and the basis of its cytoskeletal targeting.

In summary, we have cloned and characterized a new family of 350-kDa AKAPs that are the products of a multiply spliced gene region that also produces the previously described yotiao protein. In most tissues, AKAP350 localizes to the centrosome. However, in several epithelial cell types, multiple extracentrosomal foci are present. These results suggest that AKAP350 may be a multifunctional scaffolding protein.

Acknowledgments—We thank Carolyn Leithner and the Molecular Biology Core Facility for assistance with DNA sequencing, Drs. John Parente and Catherine Chew for cultured gastric parietal cells, and Julie Woodrum and Jennifer Navarre for outstanding technical assistance.

REFERENCES

1. Scott, J. D., and McCartney, S. (1994) *Mol. Endocrinol.* **8,** 5–11
2. Faux, M. C., and Scott, J. D. (1996) *Cell* **85,** 9–12
3. Theurkauf, W. E., and Vallee, R. B. (1982) *J. Biol. Chem.* **257,** 3284–3290
4. Miller, P., Walter, U., Theurkauf, W. E., Vallee, R. B., and DeCamilli, P. (1982) *Proc. Natl. Acad. Sci. U. S. A.* **79,** 5562–5566
5. Carr, D. W., Hausken, Z. E., Fraser, I. D. C., Stofko-Hahn, R. E., and Scott, J. D. (1992) *J. Biol. Chem.* **267,** 13376–13382
6. Lin, R-Y., Moss, S. B., and Rubin, C. S. (1995) *J. Biol. Chem.* **270,** 27804–27811
7. DeCamilli, P., Moretti, M., Donini, S. D., Walter, U., and Lohmann, S. M. (1986) *J. Cell Biol.* **103,** 189–203
8. Nigg, E. A., Schafer, G., Hilz, H., and Eppenberger, H. M. (1985) *Cell* **41,** 1039–1051
9. Keryer, G., Rios, R. M., Landmark, B. F., Skalhegg, B., Lohmann, S. M., and Bornens, M. (1993) *Exper. Cell Res.* **204,** 230–240
10. Vallee, R. B. (1986) *Methods Enzymol.* **134,** 104–115
11. Huang, L. J., Durick, K., Weiner, J. A., Chun, J., and Taylor, S. S. (1997) *Proc. Natl. Acad. Sci. U. S. A.* **94,** 11184–11189
12. Urushidani, T., Hanzel, D. K., and Forte, J. G. (1989) *Am. J. Physiol.* **256,** G1070–G1081
13. Dransfield, D. T., Bradford, A. J., Smith, J., Martin, M., Roy, C., Mangeat, P. H., and Goldenring, J. R. (1997) *EMBO J.* **16,** 35–43
14. McCartney, S., Little, B. M., Langeberg, L. K., and Scott, J. D. (1995) *J. Biol. Chem.* **270,** 9327–9333
15. Carr, D. W., Stofko-Hahn, R. E., Fraser, I. D. C., Cone, R. D., and Scott, J. D. (1992) *J. Biol. Chem.* **267,** 16816–16823
16. Rosenmund, C., Carr, D. W., Bergeson, S. E., Nilaver, G., Scott, J. D., and Westbrook, G. L. (1994) *Nature* **368,** 853–856
17. Gray, P. C., Johnson, B. D., Westenbroek, R. E., Hays, L. G., Yates, J. R., Catterall, W. A., and Murphy, B. J. (1998) *Neuron* **20,** 1017–1026
18. Dransfield, D. T., Bradford, A. J., Yeh, J., and Goldenring, J. R. (1997) *Biochem. J.* **322,** 801–807
19. Goldenring, J. R., Smith, J., Vaughan, H. D., Cameron, P., Hawkins, W., and Navarre, J. (1996) *Am. J. Physiol.* **270,** G515–G525
20. Komesli, S., Tournier, F., Paintrand, M., Margolis, R. L., Job, D., and Bornens, M. (1989) *J. Cell Biol.* **109,** 2869–2878
21. Marchuk, D., Drumm, M., Saulino, A., and Collins, F. S. (1991) *Nucleic Acids Res.* **19,** 1154
22. Gosti-Testu, F., Marty, M. C., Berges, F., Maunoury, R., and Bornens, M. (1986) *EMBO J.* **5,** 2545–2550
23. Chomczynski, P., and Sacchi, N. (1987) *Anal. Biochem.* **162,** 156–159
24. Berglindh, T., and Obrink, K. J. (1976) *Acta Physiol. Scand.* **96,** 150–159
25. Lewis, J. J., Goldenring, J. R., Asher, V. A., and Modlin, I. M. (1989) *Am. J. Physiol.* **258,** G476–G483
26. Tang, L. H., Stoch, S. A., Modlin, I. M., and Goldenring, J. R. (1992) *Biochem. J.* **285,** 715–719
27. Soroka, C. J., Chew, C. S., Modlin, I. M., Hanzel, D., Smolka, A., and Goldenring, J. R. (1993) *Eur. J. Cell Biol.* **60,** 76–87
28. Klauk, T. M., Faux, M. C., Labudda, K., Langeberg, L. K., Jaken, S., and Scott, J. D. (1996) *Science* **271,** 1589–1592
29. Lin, J. W., Wyszynski, M., Madhavan, R., Sealock, R., Kim, J. U., and Sheng, M. (1998) *J. Neurosci.* **18,** 2017–2027
30. Dong, F., Feldmesser, M., Casadevall, A., and Rubin, C. S. (1998) *J. Biol. Chem.* **273,** 6533–6541
31. Breer, H., Wanner, I., and Strotmann, J. (1996) *Behav. Genet.* **26,** 209–219
32. Ullrich, B., Ushkaryov, Y. A., Sudhaf, T. C. (1995) *Neuron* **14,** 497–507
33. Nadal-Ginard, B., Smith, C. W. J., Patton, J. G., and Breitbart, R. E. (1991) *Adv. Enzyme Regul.* **31,** 261–286
34. Szollosi, D. (1964) *J. Cell Biol.* **21,** 465–479
35. Stearns, T., Evans, L., and Kirschner, M. (1991) *Cell* **65,** 825–836
36. Joshi, H. C., Palacios, M. J., McNamara, L., and Cleveland, D. W. (1992) *Nature* **356,** 80–83
37. Bailly, E., Doree, M., Nurse, P., and Bornens, M. (1989) *EMBO J.* **8,** 3985–3995
38. Klotz, C., Dabauvalle, M. C., Paintrand, M., Weber, T., Bornens, M., and Karsenti, E. (1990) *J. Cell Biol.* **110,** 405–415
39. Dell'Acqua, M. L., and Scoot, J. D. (1997) *J. Biol. Chem.* **272,** 12881–12884
40. Pawson, T., and Scott, J. D. (1997) *Science* **278,** 2075–2080